On nuclear spectrometry pulses digital shaping and processing

Article *in* Measurement · July 2001

DOI: 10.1016/S0263-2241(00)00057-9

2 authors:

Cosimo Imperiale
medical technology and electronics laboratory-METEL
23 PUBLICATIONS **116** CITATIONS

SEE PROFILE

Alessio Imperiale
Institut de Cancérologie de Strasbourg Europe (ICANS)
267 PUBLICATIONS **3,455** CITATIONS

SEE PROFILE

ELSEVIER

Measurement 30 (2001) 49–73

Measurement

www.elsevier.com/locate/measurement

On nuclear spectrometry pulses digital shaping and processing

Cosimo Imperiale[a], Alessio Imperiale[b,*]

[a] *Pacific Western University, Technological Division, 600 N. Sepulveda Blvd., Los Angeles, CA 90049, USA*
[b] *Medical Technology and Electronics Laboratory, Via Potenza 18, 73100 Lecce, Italy*

Received 7 April 2000; accepted 16 July 2000

Abstract

Trapezoidal pulse shaping by a digital technique from nuclear spectrometry preamplifier output is reported. The shaping is especially suitable for time and/or pulse-height spectra measurements from high counting rate sources which commonly implies pulse pile up. In fact, piled up events may be identified and measured rather than rejected as in usual analog systems. Moreover, the amplitude-arrival time measurement of piled up pulses by the trapezoidal shape is simpler than by both maximum likelihood and least squares estimators, or adaptive nonlinear least squares methods which give better results in the case of severe pile up. Comparison with different techniques currently used in fast scanners for nuclear medicine studies is given. The technique utility in high energy semiconductor gamma ray spectrometry is also discussed.

Keywords: Pulse shortening techniques; Processing of piled up pulses at high counting rate; Pulse amplitude-time measurement; Semiconductor gamma ray spectrometry; Fast scanning for nuclear medicine studies

1. Introduction

In a semiconductor gamma ray spectrometer, the contributions to resolution are primarily due to electronic noise, statistics associated with the charge production process in the detector, and ballistic deficit (BD) arising from variations in the detector charge collection time. The system resolution is dominated by electronic noise at low energies while charge production statistics become important at somewhat higher energies, and ballistic deficit effects may become dominant at very high energies. BD effect grows when using large diameter, high efficiency detectors.

In high energy spectroscopy, when conventional spectrometric amplifiers are operated at short peaking times to achieve a high throughput rate, the variations in the detector charge collection time produce changes in amplitude which give an unacceptable photo-peak broadening [1]. In order to overcome that problem, some techniques have been proposed.

The first is the trapezoidal time-invariant shaped filter. When providing that the time when it is flat is longer than the longest charge collection time, the filter flat level is relatively immune to such rise time variations [2]. The flat top cannot be realized with lumped-parameter time-invariant filters since an infinite number of poles is required.

Delay lines have been employed to realize such a filter with fixed shaping times for short duration shaping in high energy physics [3]. Delay lines are bulky, cause severe sensitivity of gain to temperature variations, have high cost when featuring a high

*Corresponding author. Fax: +39-832-316-177.

0263-2241/01/$ – see front matter
PII: S0263-2241(00)00057-9

delay-rise time ratio, and may not easily vary in their time scale. On the contrary, variations in the time duration of the filter are required in order to optimise the signal-to-noise ratio (SNR) or the resolution against throughput rate. Therefore, they are not considered ideal circuit elements for pulse processor energy channels.

Recently, a quasi trapezoidal shape has been obtained by weighted addition of the outputs of a $\sin^8$ shaper [4]. The shape realization employs a cascade of active integrators with the highest frequency stage being the first one in the cascade. It follows that the flat top width depends on the number of stages in the cascade, the signal rise time is fixed, and long tail is present. The shape is an asymmetrical one.

The Radeka time-variant filter (Gated Integrator: GI) [2] approximates to a trapezoid by integrating (time-variant section) the output of a time-invariant prefilter, usually the output of a semigaussian shaper, and Husimi and Ohkawa filter [5] approximates to a time-variant trapezoid by weighted sum of the outputs from internal stages of a synthesized gaussian filter. If the integration time extends beyond the width of the prefilter impulse response by an amount greater than the longest charge collection time, any sensitivity to ballistic deficit is eliminated.

The GI filter is quite complex (see Note 1) and emphasizes low frequency extraneous noise sources such as microphony and power supply ripple. These factors make the filter expensive and difficult to design and to use in an optimum manner, especially when the measurement asks for a great number of gated integrators. Moreover, it produces very long dead time and is unable to correct for trapping losses.

The Harwell filter [6] removes the effects of collection time variations by starting the processing time when the detector charge is fully collected and the preamplifier output is flat. The filter presents many of the drawbacks of the GI one and, like the GI, it does not compensate for trapping losses.

On the other hand, to avoid the above mentioned difficulties and limits, BD rises when using a short peaking time unipolar semigaussian shaper without GI. If the shaper is driven by a step function with greater than zero rise time T (it is the special case in which the charge arrival times are distributed uniformly over a period T different from zero, and randomly variable from pulse to pulse), the relative BD is proportional to $(T/tp)^2$ [7], where tp is the peaking time for output with zero rise time input signal. The longer the rise time constant T of the input to the shape peaking time tp of the semigaussian signal ratio is, the longer the amplitude degradation will then be. From that, to reduce BD for applications in the gamma ray energy range >1 MeV, large coaxial detectors would be used with unipolar shapers producing output pulses peaking at 12 μs or more and therefore with total pulse widths of about 30–40 μs, which implies an unacceptable low throughput of the spectrometer. BD corrector methods have then been devised [7–12]. These methods intend to increase the spectrometer throughput yet preserving the large detector energy resolution.

Since BD is roughly proportional to $(ptd/tp)^2$, ptd being the peaking time delay which accompanies the ballistic deficit, the Goulding and Landis correcting method [8] uses the delay measurement to compensate BD. The Hinshaw and Landis method [10] is based on measuring the difference in the BD for two shapers having different peaking times, typically a unipolar semigaussian and a bipolar one. A correction based on this difference is then added to the output signal from the slower shaping channel.

In general, the Hinshaw and Landis method is better for ballistic deficit correction but quite ineffective for trapping loss correction, while the Goulding and Landis method is less effective for ballistic deficit correction but can provide excellent correction for trapping losses.

Though BD effects must be corrected in semiconductor gamma ray spectrometry, they reveal themselves to be useful in other applications. For instance, in the case that the BD of a shaping circuit output pulse is characteristic of the type of the particle, the measurement of the BD for a given input pulse realized by comparing the outputs of two shaping circuits having different shaping time constants may be used to exploit particle discrimination [13].

The above considerations apply in the case of pile up free pulse. A pile up rejector in spectrometer

pulse processors contains a fast inspection channel in parallel to the slow pulse processing one [14–17]. In the fast channel, the signals are differentiated to form narrow pulses. A fast discriminator detects such signals and produces logic signals. If a pile up is sensed by a pile up detector, the slow signal is inhibited by a linear gate. Additionally to further circuital complexity, the residual pile up time (the minimum difference in time between two successive pulses which are detectable) depends on the signal shape, the amount of superimposed noise, and both the amplitudes and the interval time between the piled up pulses. The system maximum throughout depends on the working modality of the pile up rejector. By processing pulses whose peaks occur when the previous pulse is completely finished, a 50% improvement in the maximum throughout may result [17].

Modern digital spectroscopy aims to correct rather than reject pile up events. The problem consists in measuring both the amplitude and the arrival time of piled up pulses with suitable precision and reliability, which is a difficult task. In fact, for low event rates when the pulses are isolated in time, the pulses can be very accurately detected using simple thresholding such as leading edge timing or constant fraction timing methods. For high event rates when pulse pile up occurs, these conventional methods perform poorly.

The concurrent estimation of the amplitude and the time of arrival of the signal pulse by weighted least squares (WLS) algorithm has been proposed in Ref. [18] for X-ray spectroscopy applications. Simplifications of that method aiming to reach real time digital pulse processing have been proposed in Refs. [19,20]. These algorithms are time consuming and difficult to implement in real time at high rate. Moreover, (1) the closer the peaks, the longer the estimation error will be, and (2) the concurrent estimation of the amplitude and the time of arrival uses an iterative process starting from first guess values and performing a linear approximation around them using the reference shape. The estimation difficulties increase when approaching the problem by nonlinear fitting algorithm as the Levemberg–Marquard and the Gauss–Newton ones, or, even worse, the adaptive nonlinear least squares method [21] which is more reliable than the two previous methods in the large residual case (severe pile up is present).

Let us now refer to scanners (gamma camera and position emission tomograph (PET)) for nuclear medicine studies. The scanners are complex realizations working at low energies (70–511 keV) and aiming to reach high counting rate. Count rate is important for performing dynamic studies with short lived radioisotopes for brain and cardiac studies. The scanner must be able to acquire data quickly with minimum dead time and randoms, and it must retain its intrinsic image quality. Good spatial resolution is directly linked to high image quality and the ability to visualize small structures. Good energy resolution is necessary for efficient rejection of scattered events. Pulse pile up is an important limiting factor on coincidence detection and time estimation performance in conventional and time of flight (TOF) PET [22–24] (TOF measurements are one efficient way to eliminate unwanted random and scattered coincidence events outside of a region of interest). The ability to accurately resolve temporal positions of pulses allows for improved true coincidence detection, improved accidental coincidence rejection, and, for TOF PET, improved time of flight estimates. Improvement in coincidence detection and rejection rates translate into a reduction in image artifacts and permits more accurate quantitative PET imaging.

To achieve high image and axial resolution while maintaining full organ coverage at a reasonable cost, two dimensional (2-D) detector systems in PET are employed. In most cases a 2-D array of BGO detectors is multiplexed to a small number of photomultiplier tubes (PMT); in other systems, a large crystal is coupled to a 2-D array of PMTs in an Anger-type coding scheme. All such devices that employ NaI(Tl) or BGO (position sensitive detectors) are subject to the events pile up drawback since a significant amount of time must be allowed for the integration of the scintillation light and the processing of the signal. Pile up in the 2-D detectors either results in dead time losses (in a coded system all the crystals in each module are dead when a gamma ray interacts with anyone of them) if good events pile up and are rejected by energy discriminator, or produces mispositioning of events if the composite event is

accepted[1]. The fractions of events that are mispositioned increases linearly with the amount of activity in the field of view for the configurations considered [25].

Additionally to pulse pile up, detector nonlinearities lead to significant spatial distortion, particularly near the edges of the crystal that in a complex manner degrade the quality of the reconstructed image. Position estimation is then a two-step process since the initial position estimation is followed by a spatial distortion correction [26].

Maximum likelihood (ML) estimators as position algorithms [27–31] offer advantages of improved spatial resolution and linearity over traditional position estimates in position sensitive detectors since they directly take into account the spatially varying response of the detector. Events can be localized accurately near the edge of the detector [30], which would be poorly positioned with a simple centroid calculation. This is particularly important in the determination of the axial position of the 2-D detector. Moreover, at high count rates, if two scintillations overlap in time but occur in different locations in the detector, then a centroid finding method will position the event based on an average of the two scintillation locations. The recorded location will depend on the relative intensity and the temporal relationship of the two events. The ML method is better able to identify two overlapping events and correctly locate the larger of the two.

The ML estimator, whose mean square error (MSE) is very close to the Cramer–Rao lower bound MSE (the value is intrinsic to the estimation problem independently of the estimation algorithm) has been employed to evaluate the overlap sensitivity of timing resolution with bi-exponential pulse shape from BGO-PMT detectors [32–34]. In spite of the adopted simplifications[2] the algorithm is computationally complex, and strongly dependent on the covariance estimate of the noise. In a fast version of the algorithm [35], all off diagonal terms in the weighting covariance matrix are zeroed, so leading to implement only scalar multiplications and additions instead of the complex matrix inversions used in the general estimator. But, the computing complexity reduction is obtained at a significant expense of timing resolution.

Currently, the PMT signals are digitally sampled and integrated [36,37]. Obviously, the accuracy of digitization must be sufficient to average the statistical fluctuations near the baseline where the quantization errors of each sample become significant.

To reduce the effects of pulse pile up in NaI(Tl)-based scanners, pulse shortening techniques and shortened integration time are currently used [38,39]. Pulses shortened by delay line clipped preamplifier may show signal overshoot essentially due to impedance mismatch of the cable. A pole-zero network followed by a multi-pole shaper to produce a symmetrical signal without overshoot suitable for high count rates has recently been described [40].

Whatever the pulse shortening method may be, by integrating a shorter fixed time pulse, the energy resolution may degrade because of diminished light collection as the signals are shortened for all count rate situations [38] (less than 50% of the available light is taken when integrating till a 160 ns integration time [40]).

Though the statistical resolution of the shortened integrated signal amplitude is degraded as compared to the full integration of the original pulse (the short pulse will be followed by a statistically fluctuating baseline as electrons are still released from the PMT [38]), the degree of the degradation is a function of the integration time, and is made negligibly small by

[1]GIs employ low (LT) and high thresholds (HT), analog delays, linear gate, baseline inspector and restorer circuits, pile up rejection logic, and control logic. LT fixes the integration time while HT is used for control. LT is set just above the input noise level. Whenever the shape integration is ended, the sum result is sampled and ADC converted if and only if it is higher than HT. HT cannot be selected too low to avoid system instability. But, the higher the HT level is, the greater the probability of discarding good low amplitude pulses will be. Finite stopping power due to the small detector element, non-uniform delivery of light to the PMTs, and large energy discrimination windows to compensate for poor and non-uniform energy resolution, allow many piled up events to be accepted as valid data.

[2]The search is restricted to only locations where the signal is close in Euclidean distance to the mean response. Moreover, the double photon mean and covariance functions are simply approximated by the sum of the single photon ones. These are good approximations when the overlap of the single photon responses at different times is not severe.

increasing it. From that, to improve the count rate capability of the position sensitive detector with minimum loss of resolution, the variable sampling time method was introduced [41]. Essentially, as long as the fixed time shortened pulses are widely spaced, the integration time is kept long in order to achieve good spatial and energy resolution, but if a second pulse occurs shortly after the pulse being integrated, then the integration must be terminated before the second pulse invalidates the first pulse integrated amplitude. The method realization is complex, and the maximum count rate obtainable by the above method is less than 500 kcps [42]. Moreover, since the statistical variance of a measurement point depends on the integration time, different weights are assigned to the same true value according to the pile up rate, which implies measurement errors (shifts in peak energy positions) that may not be tolerated when high resolution ADCs are employed to read the integrated level, and/or multispectral acquisition (MA) PET [43] are used (in MA PET, validation of coincident photons depends on contiguous multiple energy windows).

Techniques aiming to correct rather than reject piled up events have been presented in Refs. [44–46]. The three techniques address the pedestal and pile up problems without shortening the long tail pulses, so providing for high order pile up. The first technique [44] is designed for off-line applications. The other two techniques [45,46] are designed for gamma cameras and work in real time. In the same way as in the Tanaka method [41], a variable integration time is used here. But, while in the Tanaka method the integration time variability is realized to reduce the statistical variance of the fixed time shortened integrated pulse, in the second one it is realized to yield the maximum amount of each event light consistent with pile up. Goodness of result depends on the count rate and the pulse amplitude. In the last analysis, it depends on the effective capacity of the electronics to trigger high order piled up events at high count rates (equal or greater than 1–2 Mcps) in a reliable manner, and the integration required precision.

In this work a digital approach aiming to attenuate the above mentioned difficulties is examined. Our recent instrumentation (parallel configuration) [49] has been employed as a waveform digitizer.

2. Design concepts

In this section, the trapezoidal pulse digital shaping starting from different preamplifier time functions of major spectrometric interest will be discussed at first. The use of that pulse in amplitude-arrival time measurements, semiconductor gamma ray spectrometry, and piled up shapes' handling will be discussed later on.

2.1. Digital shaping of trapezoidal pulse

As shown in Fig. 1, a true trapezoidal pulse (TTP) may directly be synthesized by the sum:

$$vu(t) = \sum_{i=1}^{4} yi(t) \tag{1}$$

where

$$y1(t) = (A/ta)t$$

$$y2(t) = -y1(t - ta)$$

$$y3(t) = -y1(t - tb)$$

$$y4(t) = y1(t - tc).$$

The Laplace transform of (1) is:

$$Vu(s) = A[1 - \exp(-sta) - \exp(-stb) + \exp(-stc)]/(ta\, s^2)$$

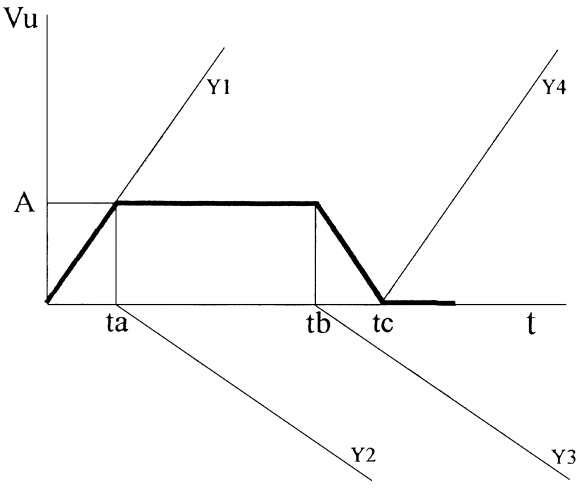

Fig. 1. Trapezoidal pulse to digitally synthesize.

and its one-sided z-transform is:

$$Vu(z) = Az(z^{nc} - z^{nc-na} - z^{nc-nb} + 1)/[na(z-1)^2 z^{nc}]$$

where, $na = ta/Ts$, $nb = tb/Ts$, $nc = tc/Ts$, $na < nb < nc$, and Ts is the sampling period.

Let us examine the transfer functions, $F(z)$, of different shapers rising the TTP at their outputs as a response to different preamplifier time functions, $vi(t)$, of major spectrometric interest.

2.1.1. $vi(t) = A\ u(t)$, the step signal of amplitude A

The z-transform of $vi(t)$ is $Vi(z) = Az/(z-1)$, so the shaper transfer function is:

$$F(z) = Vu(z)/Vi(z) = (z^{nc} - z^{nc-na} - z^{nc-nb} + 1)/[na(z-1)z^{nc}] \quad (2a)$$

$$= (z^{-1} - z^{-(na+1)} - z^{-(nb+1)} + z^{-(nc+1)})/[na(1-z^{-1})]. \quad (2b)$$

From (2b), the difference equation of the corresponding infinite impulse response (IIR) results:

$$vu(k) = vu(k-1) + (1/na)[vi(k-1) - vi(k-na-1) - vi(k-nb-1) + vi(k-nc-1)].$$

From (2a), $F(z)$ may be written as

$$F(z) = \left(\sum_i z^{-i} - \sum_j z^{-j}\right)\Big/ na \quad \begin{matrix} i = 1, 2, 3, \ldots, na \\ j = nb+1, nb+2, \ldots, nc \end{matrix}$$

so, the difference equation of the corresponding finite impulse response (FIR) results

$$vu(k) = \left[\sum_i vi(k-i) - \sum_j vi(k-j)\right]\Big/ na.$$

2.1.2. $vi(t) = A\ \exp(-t/\tau)$, the single exponential signal with amplitude A and time constant τ

The z-transform of $vi(t)$ is $Vi(z) = Az/(z - \exp(-Ts/\tau)) = Az/(z-e)$, where $e = \exp(-Ts/\tau)$, so the shaper transfer function is

$$F(z) = [z^{nc+1} - z^{nc-na+1} - z^{nc-nb+1} + z - e(z^{nc} - z^{nc-na} - z^{nc-nb} + 1)]/[na(z^{nc+2} - 2z^{nc+1} + z^{nc})] \quad (2c)$$

and the IIR difference equation

$$vu(k) = 2vu(k-1) - vu(k-2) + \{vi(k-1) - vi(k-na-1) - vi(k-nb-1) + vi(k-nc-1) - e[vi(k-2) - vi(k-na-2) - vi(k-nb-2) - vi(k-nc-2)]\}/na.$$

2.1.3. $vi(t) = A\ (\exp(-t/\tau_1) - \exp(-t/\tau_2))$, the biexponential pulse shape with τ_1 the scintillator light decay constant and τ_2 the PMT rise time constant

The z-transform of $vi(t)$ is $Vi(z) = Az(a-ab)/((z-a)(z-b))$, where $a = \exp(-Ts/\tau_1)$ and $b = \exp(-Ts/\tau_2)$. The shaper transfer function is then

$$F(z) = (z-a)(z-b)(z^{nc} - z^{nc-na} - z^{nc-nb} + 1)/[na(a-b)z^{nc}]. \quad (3a)$$

From now on and till further notice, the signal amplitude will be expressed on the scale of 12-bit ADC LSB unit, the amplitude being normalized to one, and the time on the scale of the sampling period $Ts = 5$ ns.

Fig. 2a shows two noisy (noise std = 4LSB), 100LSB high, 250-ns time constant exponential signals piled up with an interval time between the two pulses equal to $60Ts$.

Fig. 2b and c shows the shaped trapezoidal signal in the case of $ta = 50$ ns, $tb = 150$ ns, $tc = 200$ ns, and its derivative, respectively. Analogously to Fig. 2, Fig. 3 shows the shaped signal and its derivative in a more severe pile up situation; the interval time between the two pulses is now $15Ts$, even the shortened signals getting involved in the pile up process.

From the above results, it follows:

1. Shortening long pulses by digital shapers, the (2a) transfer function implementation being the simplest one, avoids delay line drawbacks.
2. Both the leading and the trailing edge slopes, as well as the flat top width of the synthesized

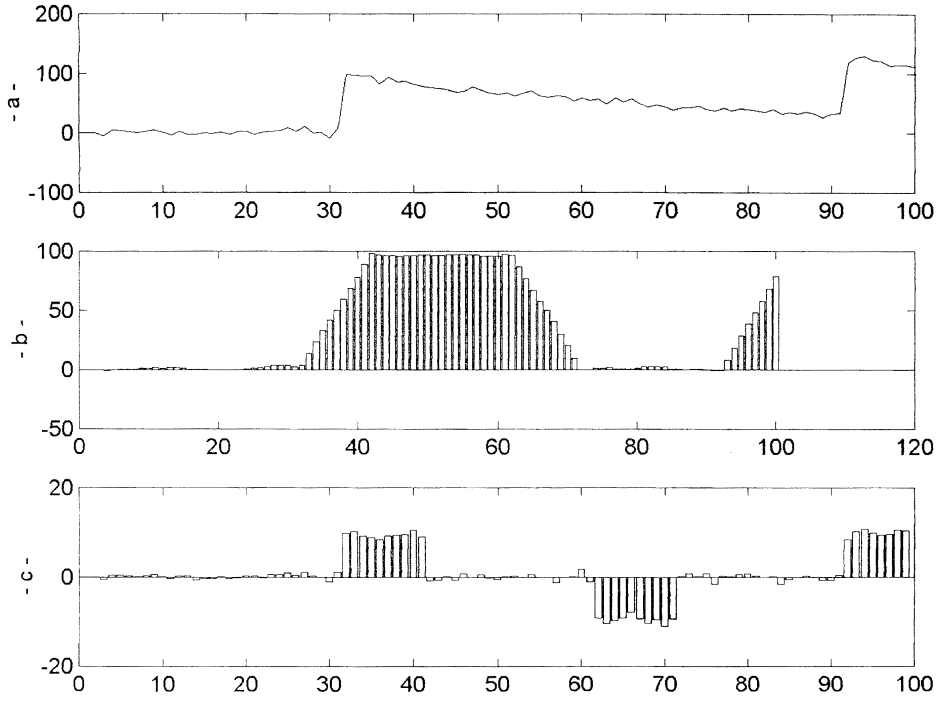

Fig. 2. 200 ns width trapezoidal shape synthesized from two noisy piled up pulses with 300 ns inter-arrival time.

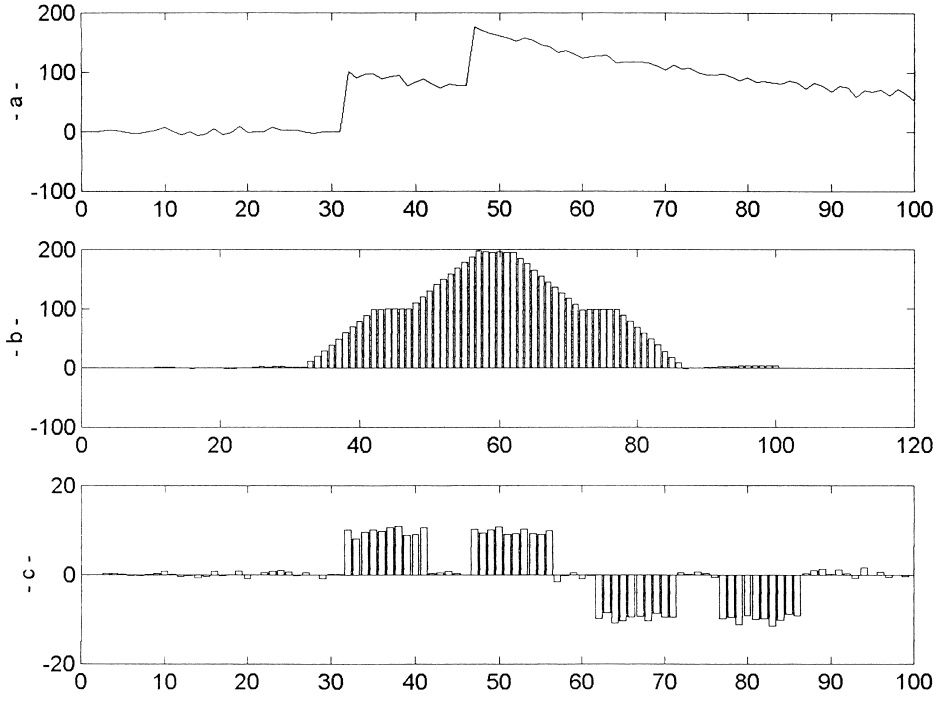

Fig. 3. As Fig. 2 with the exception of the time interval between the two piling pulses (75 ns).

trapezoidal pulse are programmable. The shape may then be used in a wide range of spectrometric measurements.

3. Thanks to the multi-pole structure characterizing the transfer functions, the trapezoidal shape has no droop on its top and, at least in the ideal case, no edge distortions. That result may unlikely be obtained by analog techniques approximating the ideal shape, in spite of the optimization procedures applied to some analog multi-pole structures [47].

2.2. Pulse amplitude-arrival time measurement

The amplitude and the arrival time of the pulse may easily be measured by averaging the flat-top values and computing the zero crossing time of the least squares line interpolating the points which belong to its leading edge, respectively.

Computing complexity concerning WLS, ML, median filtering and spline smoothing [48] methods is so avoided. Incidentally, median and spline filtering may worsen both amplitude and edges of the spectrometric signal especially when dealing with sharp, low amplitude peak signals.

Flat-top value averaging reduces the noise standard deviation of the single realization at the shaper output by the quantity $\sqrt{N}$, N being the number of averaging points. The shaper output noise std (shpstd) depends on the noise std from the preamplifier (pstd) and the time parameters of the trapezoidal signal. For instance, some shpstd values obtained by 20,000 repeated measurements are as follows:

shpstd = 0.711 pstd, for $Ts = 5$ ns, $ta = 20$ ns, $tb = 80$ ns, $tc = 100$ ns;

shpstd = 0.450 pstd, for $Ts = 5$ ns, $ta = 50$ ns, $tb = 150$ ns, $tc = 200$ ns;

shpstd = 0.304 pstd, for $Ts = 50$ ns, $ta = 1$ μs, $tb = 3$ μs, $tc = 4$ μs.

Whatever the signal amplitude, the estimation of the pulse arrival time by the zero-crossing time of the least squares line gives better results compared to the classical threshold crossing time estimator (the time std of the threshold crossing — time jitter — is obtained by dividing the signal std amplitude by the slope of the signal at the crossing time), goodness of result depending on the signal leading edge sample numbers, too. In fact, if the input signal is a non-zero rise time step, the trapezoidal signal from the shaper (2a) will be delayed depending on the step rise time value and its edges will be base broadened and top tightened (Fig. 4). Nevertheless, the pulse flat top quality is preserved and, provided that both the amplitude and the number of samples characterizing the signal edges are sufficiently high, the nonlinear zones of the edges may easily be located and left out of the least squares line computing without jeopardizing goodness of result even in noisy signals.

In respect of the estimation of the pulse arrival time, the step non-zero rise time drawback turns into an advantage. In fact, by event non-synchronized sampling modality, the time of arrival of a perfect step signal may be estimated with an accuracy stated by the sampling interval. On the contrary, by the same modality, non-zero rise time step signal arrival times which are submultiples of the clock period may be estimated with very low jitter.

Figs. 5 and 6 synthesize the jitter measurement results in the case of 4LSB std noise at the input of the shaper and different pulse widths. Fig. 5 refers to the Fig. 2b pulse, while Fig. 6 refers to a 10-μs-width pulse with $ta = 2$ μs, $tb = 8$ μs, $tc = 10$ μs, and $Ts = 100$ ns. The method is particularly effective at low signal amplitudes.

The digitally synthesized trapezoidal pulse is then very useful, for instance, in coincidence measurements, especially in high rate TOF ones, time-to-amplitude conversion (TAC) techniques being generally prohibitive at MHz start rates. Our instrumentation [49] overcomes that problem too in time-amplitude measurements of pulses from fast analog GIs. The digital approach is able to measure arrival times which may be submultiples of the clock period with very low jitter without the typical drawbacks associated with triggering in analog systems (comparator slew time, temperature variability and inter-channel unmatching of propagation delay, TAC conversion errors), and, as it will be shown later, also in the case of severe pile up.

A trigger may yet be used to start the pulse shaping, but in that case its time precision would not

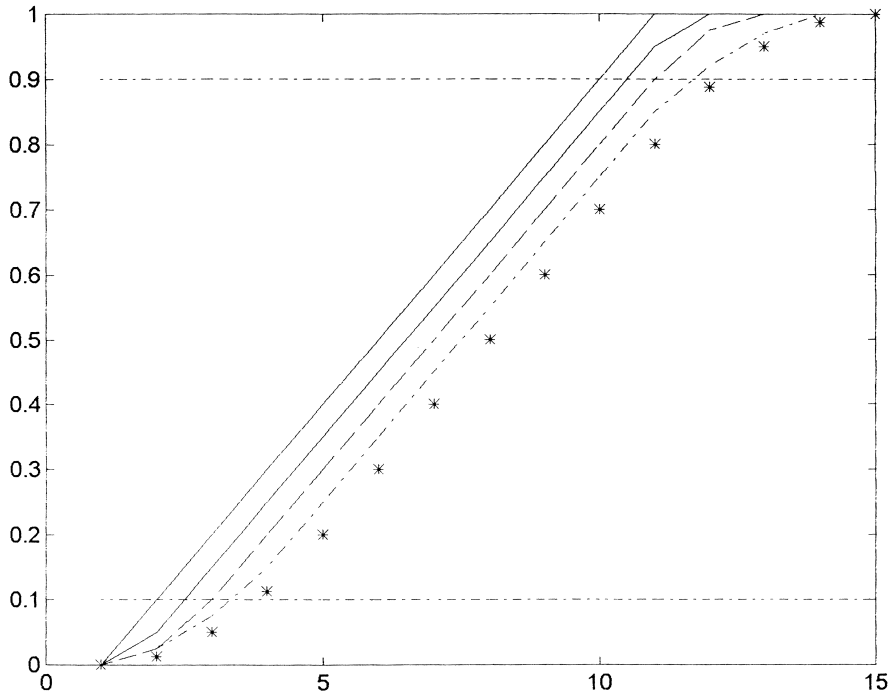

Fig. 4. Normalized trapezoidal shape first edge for different rise times of the input step. From left to right, the first line is the filter response to zero rise time step. The second and third lines are the responses to 10 ns rise time step when the sampling clock and the step are perfectly synchronised, and the step is delayed by an amount equal to 0.5*Ts*, respectively. The fourth and fifth lines corresponding to 20 ns rise time step, have analogous meaning. Horizontal axis quotes time scaled in sample number.

be a fundamental requirement since the trigger would mainly be used for the sake of reducing the amount of data to be processed. The input signal is continuously sampled. The samples are stored in a buffer memory of suitable fixed depth, mainly determined by the selected shaper difference equation, updating at each new sample. On the arrival of a trigger signal, the words already stored in the buffer memory in addition to the next acquiring ones will take part in the signal shaping.

If the shaper input signal is a biexponential one, the lack of synchronisation between the signal and the sampling clock raises error in the measurement of the shaped trapezoidal pulse flat top level. That error increases with shortening the τ_2 time constant for selected values of the τ_1 time constant and the sampling clock period *Ts*. Fig. 7 shows the flat-top amplitude errors concerning amplitude normalized biexponential signals with $\tau_1 = 250$ ns and $Ts = 5$ ns for different time delay between the event and the sampling clock, and different τ_2 values ($\tau_2 = 20$, 40 and 80 ns, respectively), the maximum error occurring when the delay is equal to $1/2Ts$. It is lower than one 12-bit LSB for $\tau_2 = 80$ ns while it is lower than one 11-bit LSB and 10-bit LSB for $\tau_2 = 40$ ns and $\tau_2 = 20$ ns, respectively. Obviously, at equal sampling interval, the result worsens for τ_2 values shorter than 20 ns becoming the worst in the case of exponential signal which shows maximum asymmetry.

An obvious way of reducing the synchronisation error consists in shortening the sampling time interval. For instance, a biexponential signal with $\tau_1 = 250$ ns and $\tau_2 = 20$ ns shows flat top maximum error of 156 μV and 25 μV when sampled at 2.5 ns and 1 ns, respectively. Analogously, a biexponential signal with $\tau_1 = 250$ ns and $\tau_2 = 5$ ns shows a maximum error of 2.5 mV when sampled at $Ts = 5$ ns, and a maximum error less than 400 μV when sampled at $Ts = 2$ ns. Unfortunately, the powerful and low cost 500 MHz waveform digitizers at present commercially available (for instance, the Signatec PDA500

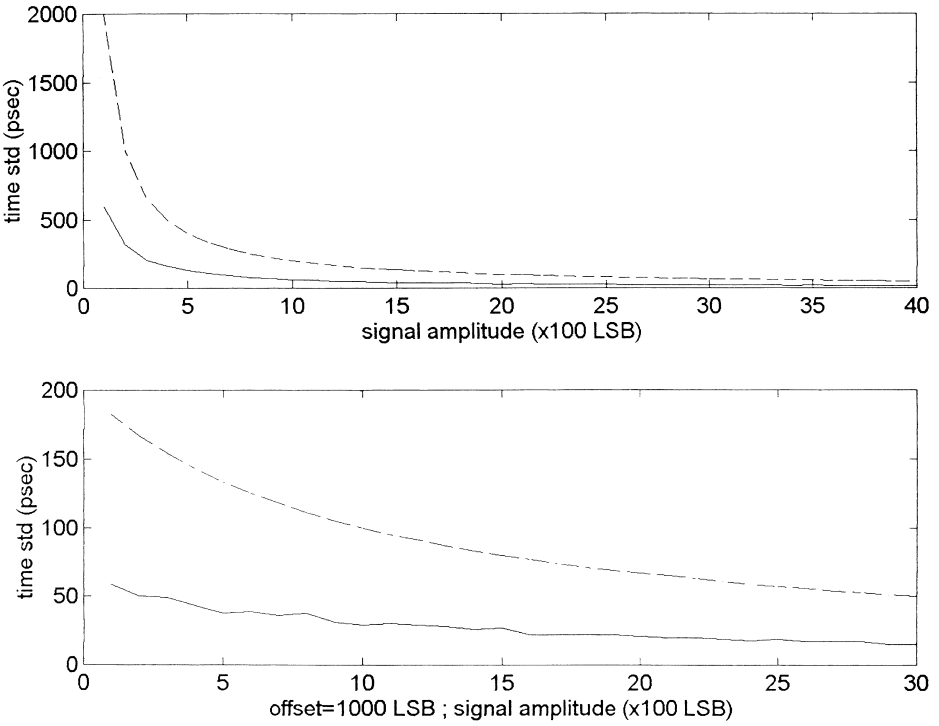

Fig. 5. Time jitter corresponding to different signal amplitudes of the 200 ns width symmetric trapezoidal pulse with 50 ns rise time. —, result by the present method; - - -, result by the threshold crossing time estimator.

PCI board), are equipped with 8-bit resolution ADC. So, when feasible, a cheap way of obtaining 12-bit precision result consists in applying a correction factor depending on time delay measurement to the measured flat top level. Otherwise, a precise trigger is mandatory.

2.3. Semiconductor gamma ray spectrometry

Resolution enhancement circuits in semiconductor gamma ray spectrometry rely upon accurate time and amplitude measurements to compute their correction, and may introduce new error sources.

For instance, by using the same notation of the Introduction, a correction proportional to $(td/tp)^2$ implies an error term proportional to $(td/tp)^4$ [12], which may be neglected only if $td \ll tp$. To reduce the error term, relatively long *tp* values must then be used, the *tp* value depending on the required energy resolution. Provided that condition is satisfied, the shaping of the signal correcting for charge trapping loss, the correction signal being summed to the peak value of the pile up free pulse, asks for complex analog circuits [8,9,12] either in the case of simple correcting quadratic law or different power one. Moreover, the *tp* value may not directly be measured and the peak identification is always a difficult problem (with negligible superimposed noise, the 14-bit and 12-bit resolution peak amplitude identification of a 6th order semigaussian shape with 1 μs shaping time, implies a time indetermination of about 40 ns and 120 ns, respectively, which lowers to about 10 ns and 40 ns when using a shaping time equal to 250 ns).

Essentially, the above correcting analog systems compute the correction $So \times td^n$ instead of the $So \times tcoll^n$, where *So* is the peak amplitude for zero signal rise time, *tcoll* is the carriers charge collection time, and $1.5 \leq n \leq 3$ ($n = 2$ in Ref. [8]). But, the preamplifier signals are known to not rise linearly, so the relation between *tcoll* and *td* is not linear. It is

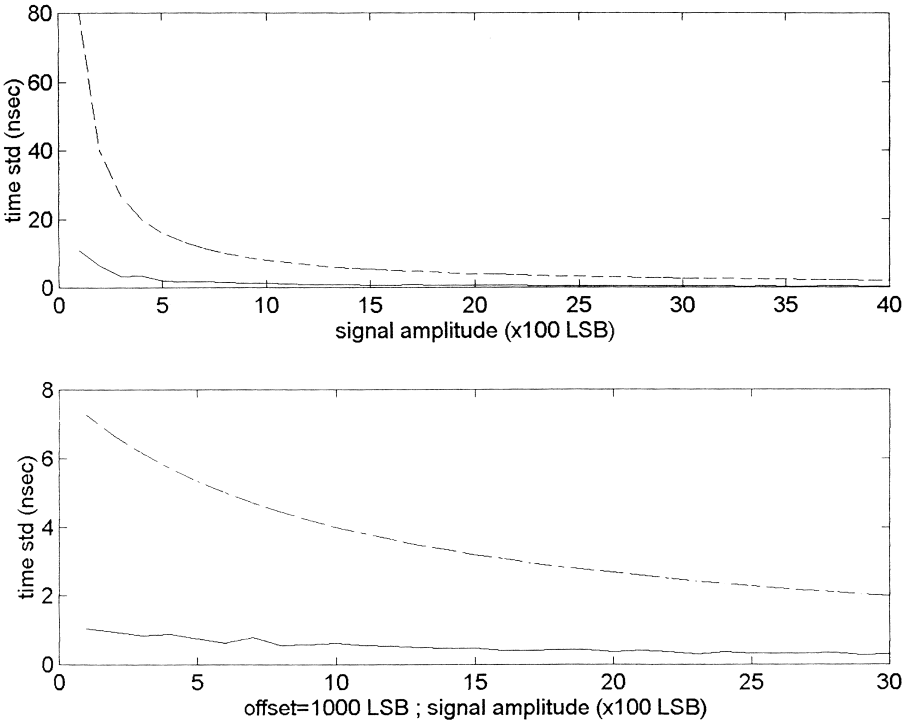

Fig. 6. As Fig. 5 with the exception of the pulse time characteristics (10 μs width, 2 μs rise time).

approximately linear when the interaction occurs at a distance $r > 0.4(r1 + r2)$, $r1$ and $r2$ being the radii of the inner and outer detector contacts. Since more than 80% of the interactions occur for $r > 0.4(r1 + r2)$, a majority of the signals from the detector so receive the proper correction while a small number are overcorrected. The situation worsens in the case of multiple interactions in the detector.

Recently [50], to avoid confusion between trapping and ballistic deficit effects when applying a correction to signals based on any rise time determination, the analog flat topped pulse shaper [4] that makes BD effects negligible is used in the energy measuring channel while a parallel channel implements a statistical correction for trapping loss. The parallel channel locates full energy events at different radii in pure coaxial geometry germanium detectors by measuring the peak time of the detector current pulses, the peak current time being almost linearly related to the radius. A radius-dependent peak position correction is then applied to improve the spectrometer resolution. Apart from the working condition and statistical approach on which the design is founded, the resultant circuit is complex requiring peak finder circuit, TAC, pulse height analyzer and associated routing logic to sort the energy signals in a number of groups according to the peak time value.

The shaping of trapezoidal pulses by digital technique requires the sampling of the signal at the preamplifier output, so both the arrival time and *tcoll* can be measured directly and precisely, provided that the sampling frequency is sufficiently high (the time of a rising edge crossing a particular amplitude level can be deduced from the linear interpolation of the two nearest samples). Incidentally, though *tcoll* may directly be measured by the trapezoidal shape edge, multiple interactions in detector, preamplifier bizarre nonlinear rise, and the composition rule of delay times make the measurement result less reliable than the one obtained by the preamplifier output. The above information can be utilized besides trapping correction for other purposes; for instance, to estimate the shape distribution of pulses from the

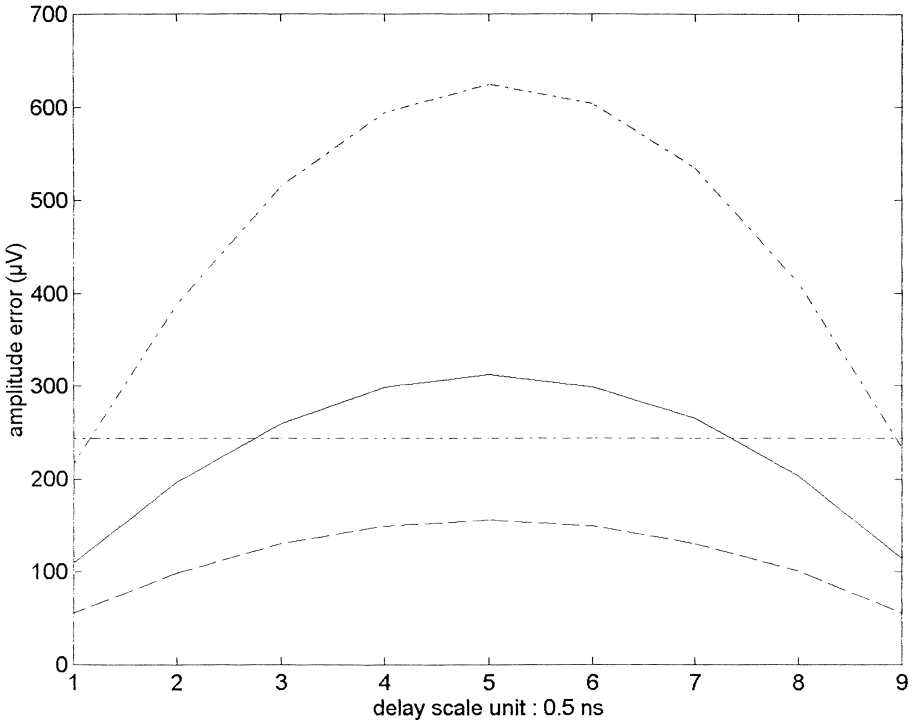

Fig. 7. Amplitude error at the output of the trapezoidal shaper as function of the sampling clock ($Ts = 5$ ns)-event delay, corresponding to biexponential shapes with different shaping time constants at the shaper input. – · –, $\tau_2 = 20$ ns; —, $\tau_2 = 40$ ns; - - -, $\tau_2 = 80$ ns; -·-·-, horizontal line: one 12-bit LSB.

detector without complex measurement electronic systems [51–53].

Both flexibility in time parameters selection and energy level achievable precision are two further elements for the digital technique. In fact, noise may be negligible in very high energy applications, but it may not be true when the spectrometer has to measure a wide range of energy. In this case, by using semigaussian shape-based analog systems, noise spikes may flag a false peak rather than the true pulse peak so jeopardizing the measurement result in spite of the means that the present fast, powerful 12-bit and 14-bit sampling ADCs (SADC) offer. That drawback is attenuated by both analog trapezoidal shape and digital systems [36] in which the peak indication is verified by a prefixed number of subsequent comparisons. At high resolution, the second solution is not reliable and is time consuming. The first solution implies the acquisition, by sampling, of one flat top point of the noisy signal so that, to reduce the flat top level reading error due to noise, relatively long peaking times must be employed for a selected pulse width (that is now the only need for long peaking time since the use of analog trapezoidal shape no longer asks for long peaking time to reduce the error in the BD correction). But, the condition of minimum noise for a time invariant trapezoidal signal [54] implies a relatively long pulse width with detriment to the system throughout and rise in pile up probability.

By the trapezoidal pulse synthesis digital technique, the pulse leading edge width is determined by both *Ts* and the number of points employed to take out the signal and the necessary time information while the minimum pulse flat top width is determined by the detector response. It being understood that both conditions must simultaneously be satisfied, the pulse may be shortened compatibly with those conditions. Owing to signal time parameter programmability and the always optimum response of

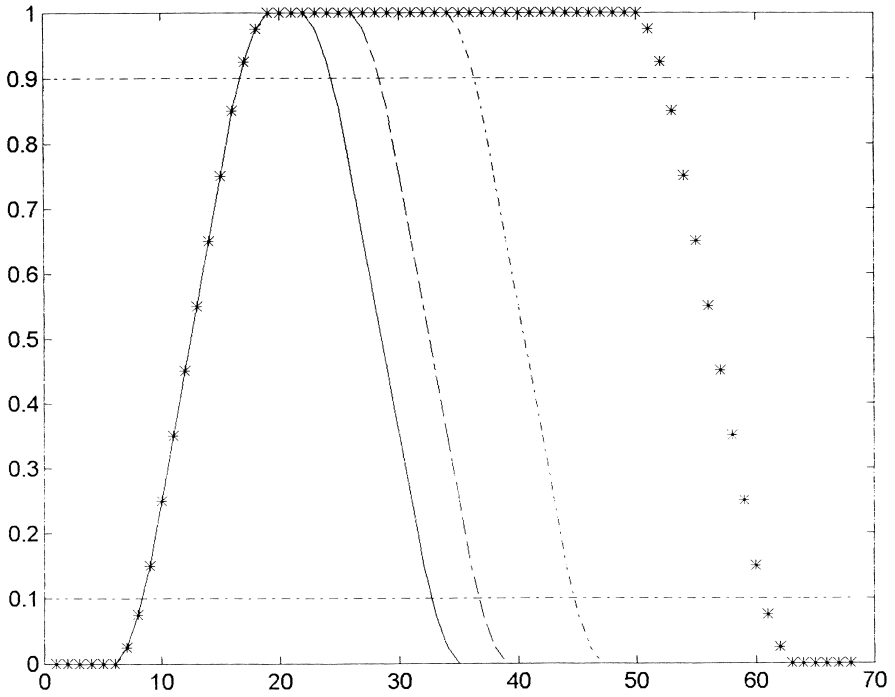

Fig. 8. Shaper responses to 500 ns rise time input step for different programmed flat top widths. Horizontal axis quotes time scaled in sample number. *Ts* = 100 ns. —, 600 ns; - - -, 800 ns; – · –, 1200 ns; **, 2000 ns.

the shaper with changing those parameters (Fig. 8), the higher noise resulting from shortening may be compensated by increasing the number of flat top points taking part in the averaging which will reduce the noise variance of the flat top level result. Let us note in this connection that the finite rise time of the preamplifier output signal reduces the flat top points programmed number.

2.4. Handling of piled up pulses

The trapezoidal shaper digital synthesis is also advantageous when handling piled up pulses at high counting rate. The table in Fig. 9 synthesizes the percent rates of piled up pulses of different order $w(i)$, $i = 1–4$, at different high mean counting rates and different time intervals. Let us refer to the table results and to high rate NaI(Tl)-based scanners in which, owing to the long scintillator light decay time constant (250 ns), the pile up effect is the most limiting factor to their counting rate capability.

By methods acting without shortening the long tail

μ Mean rate (Mcps)	$\delta\tau$ Time interval (ns)	Per cent of piled pulses			
		W(1)	W(2)	W(3)	W(4)
1	0 - 50	4.75	0.12	0.002	
	50 - 150	8.16	0.85	0.048	
	150 - 200	3.46	0.67	0.050	
	Σ	16.37	1.64	0.10	
2	0 - 50	9.00	0.45	0.015	0.00038
	50 - 150	13.22	2.88	0.315	0.025
	150 - 200	4.58	2.03	0.390	0.047
	Σ	26.80	5.36	0.720	0.072
3	0 - 50	12.91	0.97	0.05	0.0018
	50 - 150	15.78	5.49	0.92	0.0982
	150 - 200	4.24	3.42	1.01	0.2
	Σ	32.93	9.88	1.98	0.3000
4	0 - 50	16.37	1.60	0.10	0.005
	50 - 150	16.56	8.28	1.88	0.295
	150 - 200	3.01	4.50	1.85	0.470
	Σ	35.94	14.38	3.83	0.770

Fig. 9. Percent rate of piled pulses from Poisson statistics at different mean counting rates and time intervals.

pulse, the percent rate of high order pile up is not at all negligible at high counting rate ($w(1) = w(2) = 27\%$, $w(3) = 18\%$, $w(4) = 9\%$ and $w(1) = 7\%$, $w(2) = 15\%$, $w(3) = w(4) = 20\%$, $w(5) = 16\%$, $w(6) = 10\%$ for $\delta t = 1$ μs, $\mu = 2$ Mcps and 4 Mcps, respectively), and the amount of first order pile up is already high in the first 50-ns interval. Supposing the integrating signal amplitude is sufficiently high to realize the difference from noise, if the trigger is not 100% efficient, the result of the light integration between the next two pulses will suffer from errors which sum up in the course of computing, the time interval between the next two pulses being a component of the computing result [46]. By shortening the pulse from the trapezoidal shaper to about 100 ns width (the maximum width of the first order piled up pulse is twice the width of the nonpiled shaped pulse), the counting loss due to second order pile up may still be high at high counting rate, but the recovery of the first order piled up pulses is a more significant result even in comparison with the ML one which identifies two overlapping events correctly locating the larger of the two.

Systems which employ delay line clipping preamplifier [41] or charge preamplifier with shaping stages to perform pulse shortening without pulse overshoot [40], must be pile up free in the course of the light integration process, so, in addition to the light lost for shortening, a great amount of pulses is not counted in spite of the shortened pulse width (100–200 ns). Digital integration of the shortened pulse [36,37,40] performed by using short *Ts* is however advantageous either to reduce jitter which is high in the actual systems [40] or to have an appropriate number of points to average the values of the noisy level of the signal integrated for a time longer than the pulse width, yet taking short the overall dead time.

As shown in Fig. 2b and Fig. 3b, the digitally synthesized trapezoidal shaper needs neither trigger nor pile up inspector/rejector circuits. Moreover, working on a signal from either a suitable charge preamplifier [40] or realistic biexponential signal directly taken from PMT anode, the shaper is immune from the light reduced collection drawback. By increasing the counting rate, short signals from the preamplifier are advantageous to decrease the order of pile up earlier in the shaping process.

Figs. 10 and 11 show two samples of the same biexponential shape from the preamplifier (peaking time and maximum width at 12-bit resolution of the normalized shape are 60 ns and 780 ns, respectively. The sampling time is 2.5 ns) working at 1 Mcps and 2 Mcps mean rate, respectively, and the corresponding trapezoidal shaper outputs. The edges of the non-piled up trapezoidal pulse are quite linear. A suitable high threshold avoids the system saturation owing to pile up.

Let us say *tdel*, *Tr*, and *Tft* are the interval time between the edges of two piled events, and the nonpiled shape widths of the leading edge and the flat top, respectively.

By symmetrical trapezoidal shape, the possible first order pile up events are as follows:

1. $tdel = ta$.

   The piled up shape shows only a flat top. Two non-zero clusters separated in time by a statistically zero cluster with width equal to the flat top one are characteristic of the shape derivative.

   If the two piling pulses are of equal amplitude (Fig. 12a), the flat top width of the piled pulse is the half of the non0piled pulse one while the number of elements of each non-zero cluster is twice the number of the non-piled pulse. The elements of each cluster are characterized by statistically equal amplitude, and the flat top level amplitude is equal to the sum of the two non-piled flat top levels.

   On the contrary (Fig. 12b), the flat top level amplitude is again equal to the sum of the two nonpiled flat top levels. The amplitude of the first pulse as well as the arrival time of the second one are determined by the point of intersection of the two least squares lines characterizing the leading edge of the piled pulse.
2. $ta < tdel \leq 2ta$.

   The piled up shape shows three flat tops. The first and the last flat top levels (from left to right) are the statistically true ones of the two piling pulses. The second flat top level is equal to the sum of the other two levels (Fig. 13). The number of points belonging to that level is reduced as delay increases to become only one when $tdel = 2ta$. Though pile up does not deteriorate the signal edges, the computing of the arrival times of the

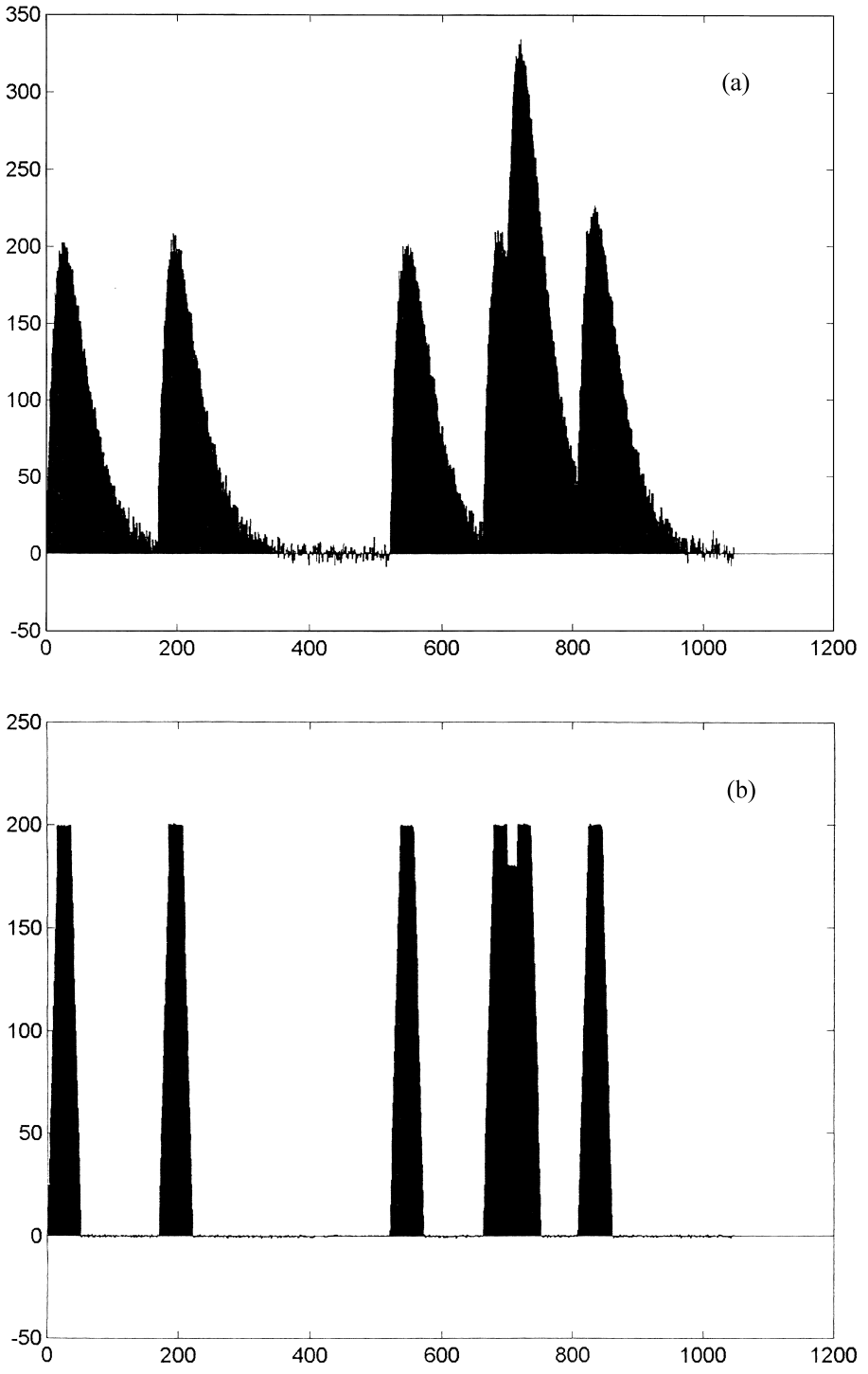

Fig. 10. Trapezoidal shaper response (b) to piled up biexponential pulses (a) at 1 Mcps mean counting rate. (c) and (d) show the fourth response and its derivative in detail. Even the shortened pulses are piled up. Horizontal axis quotes time scaled in sample number ($Ts = 2.5$ ns) while the vertical one shows the signal amplitude scaled in number of 12-bit LSBs.

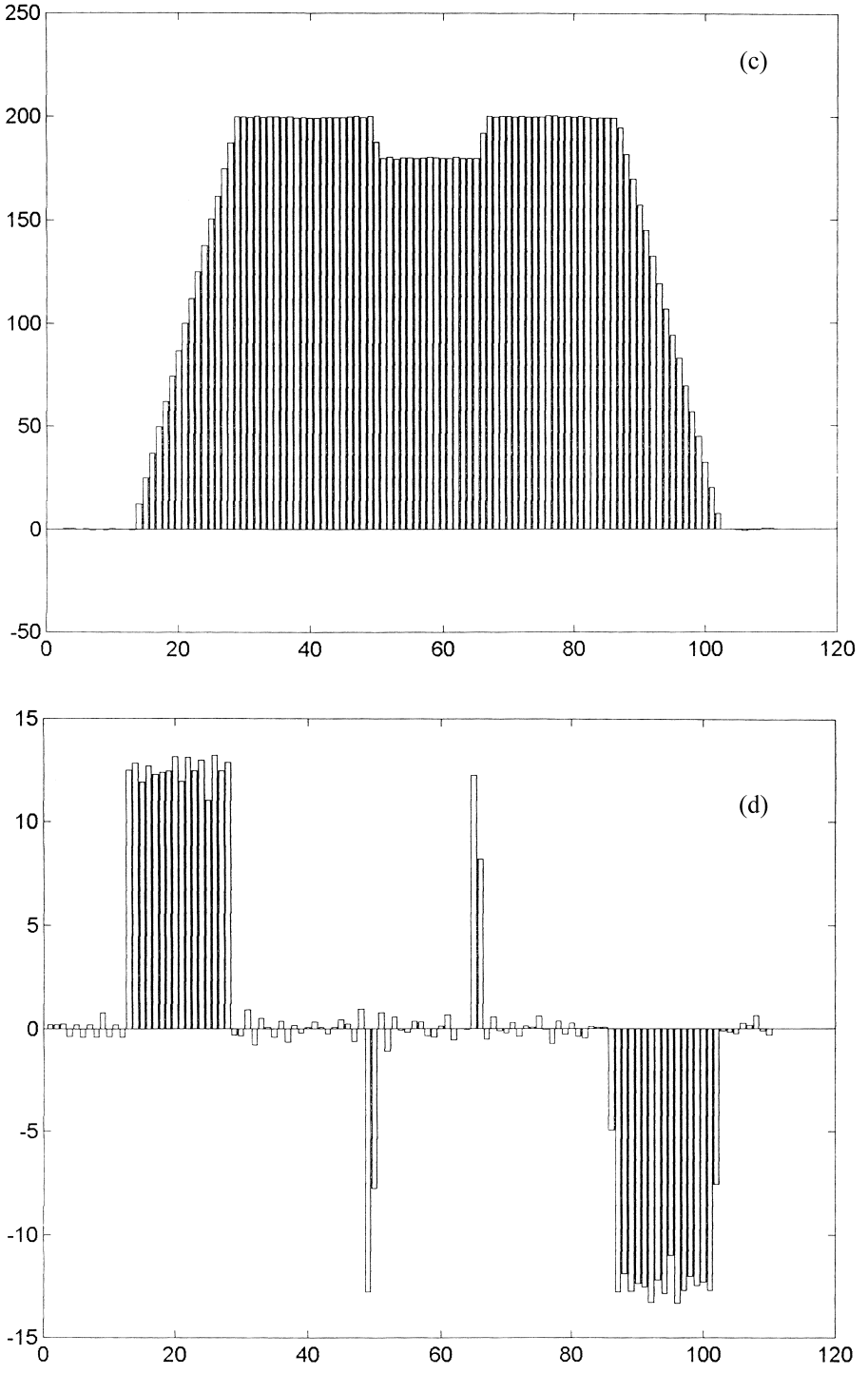

Fig. 10. (*continued*)

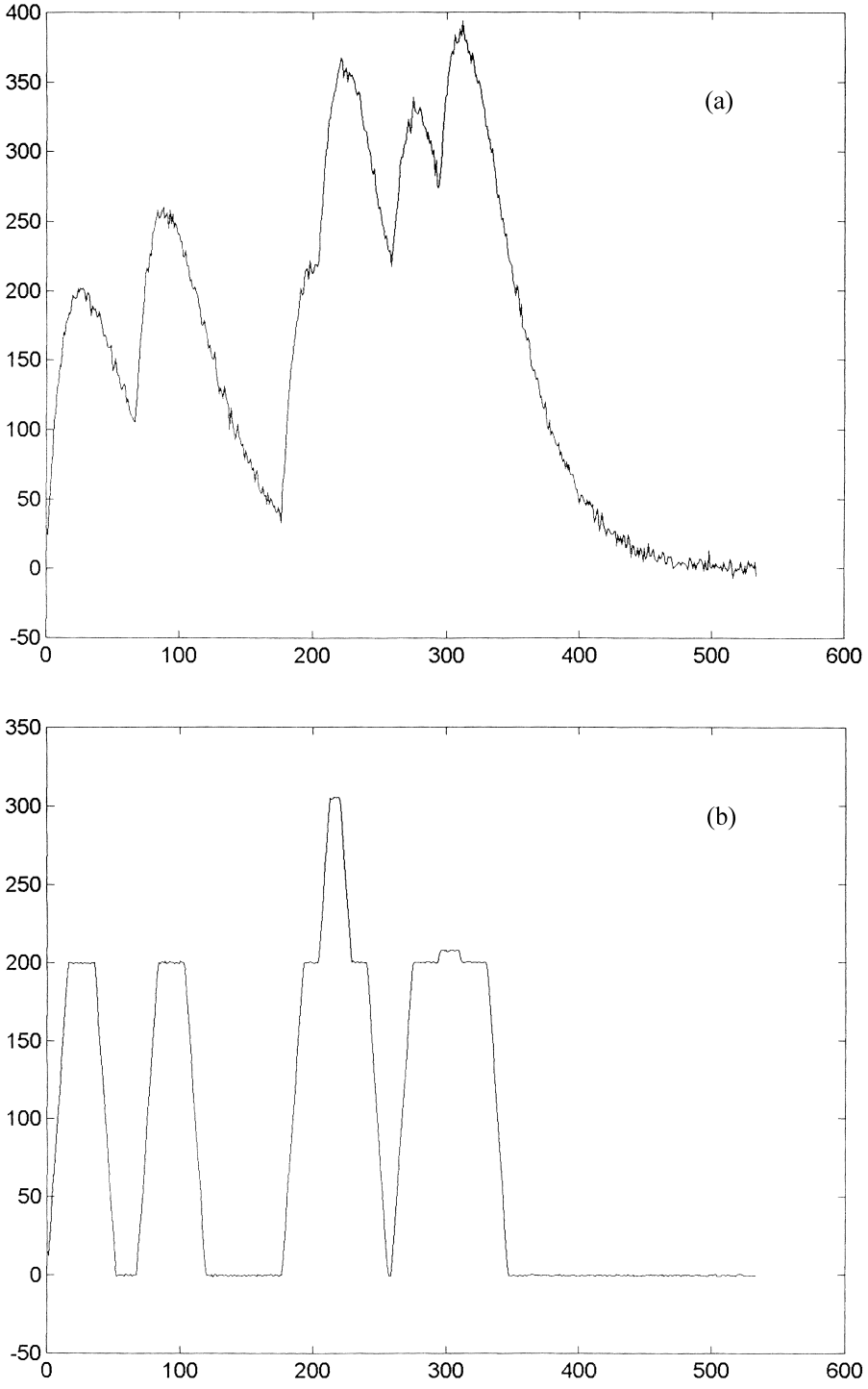

Fig. 11. As Fig. 10 except for the mean counting rate which is here equal to 2 Mcps. (c) and (d) show the third and the fourth shaper responses in detail.

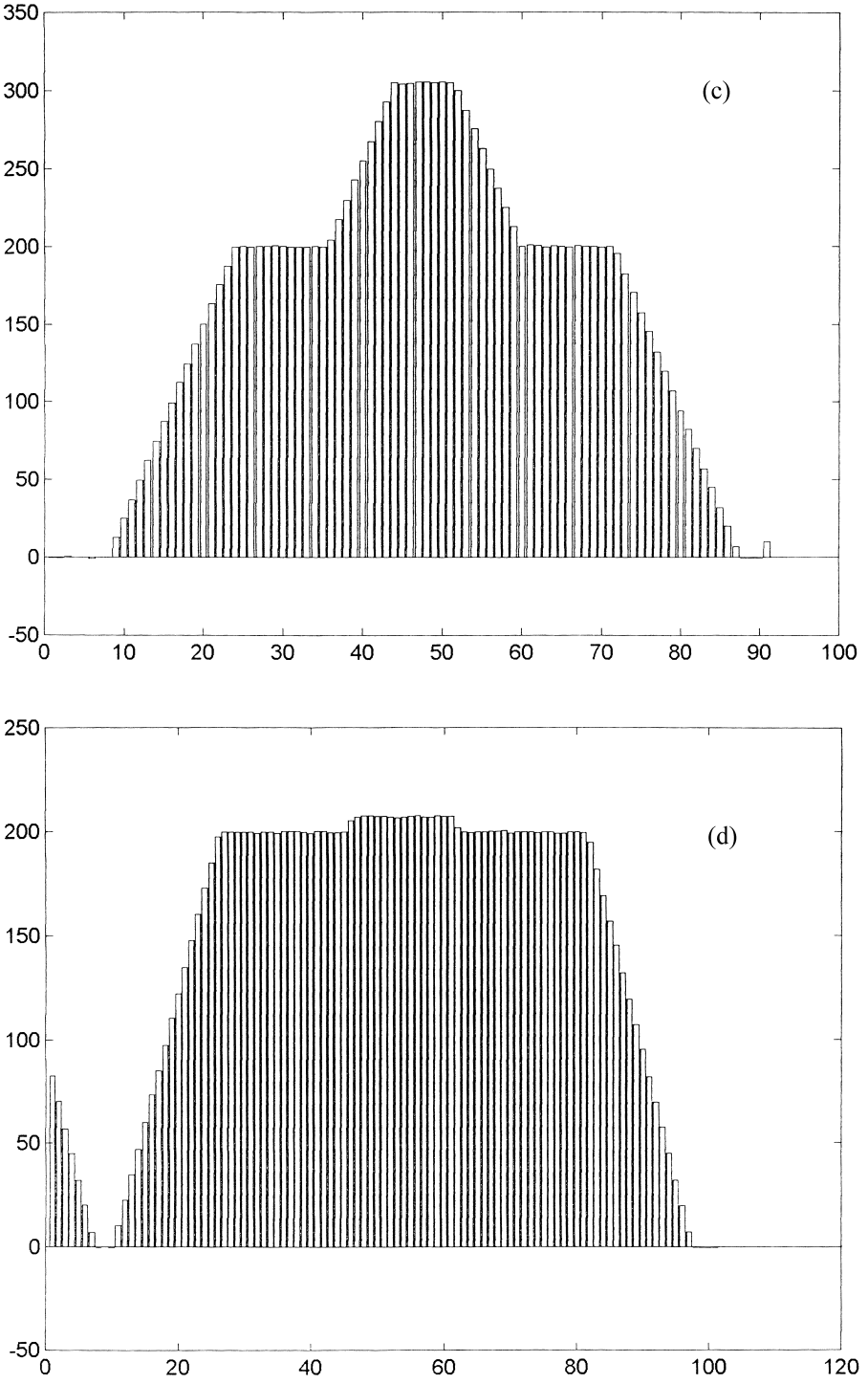

Fig. 11. (*continued*)

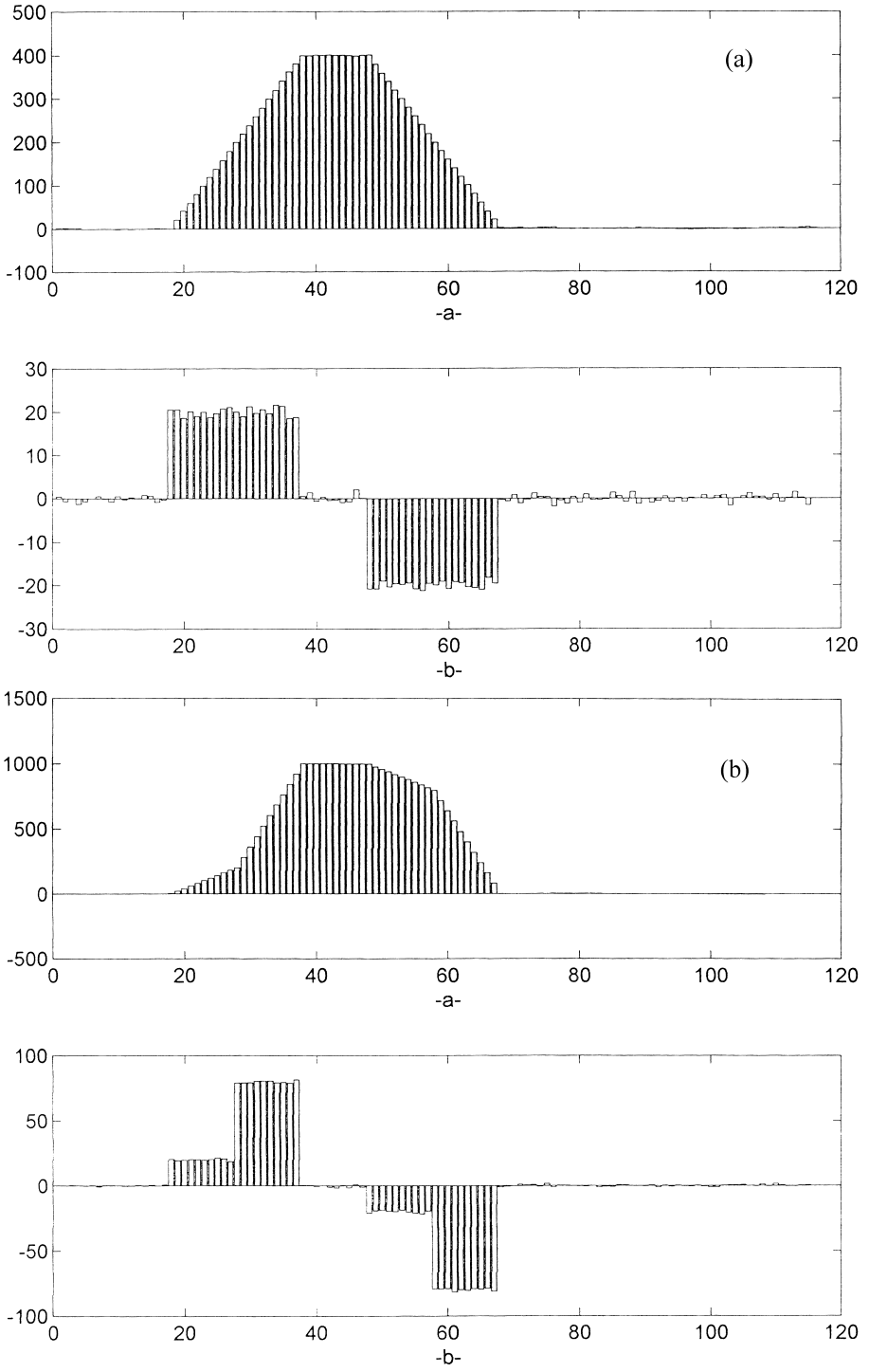

Fig. 12. Trapezoidal shaper output in the case of first order pile up with $tdel = ta$ ($Ts = 5$ ns, $ta = 10Ts$). In (a) the two piling up signals have equal amplitude (200LSB) while in (b) they have different amplitude.

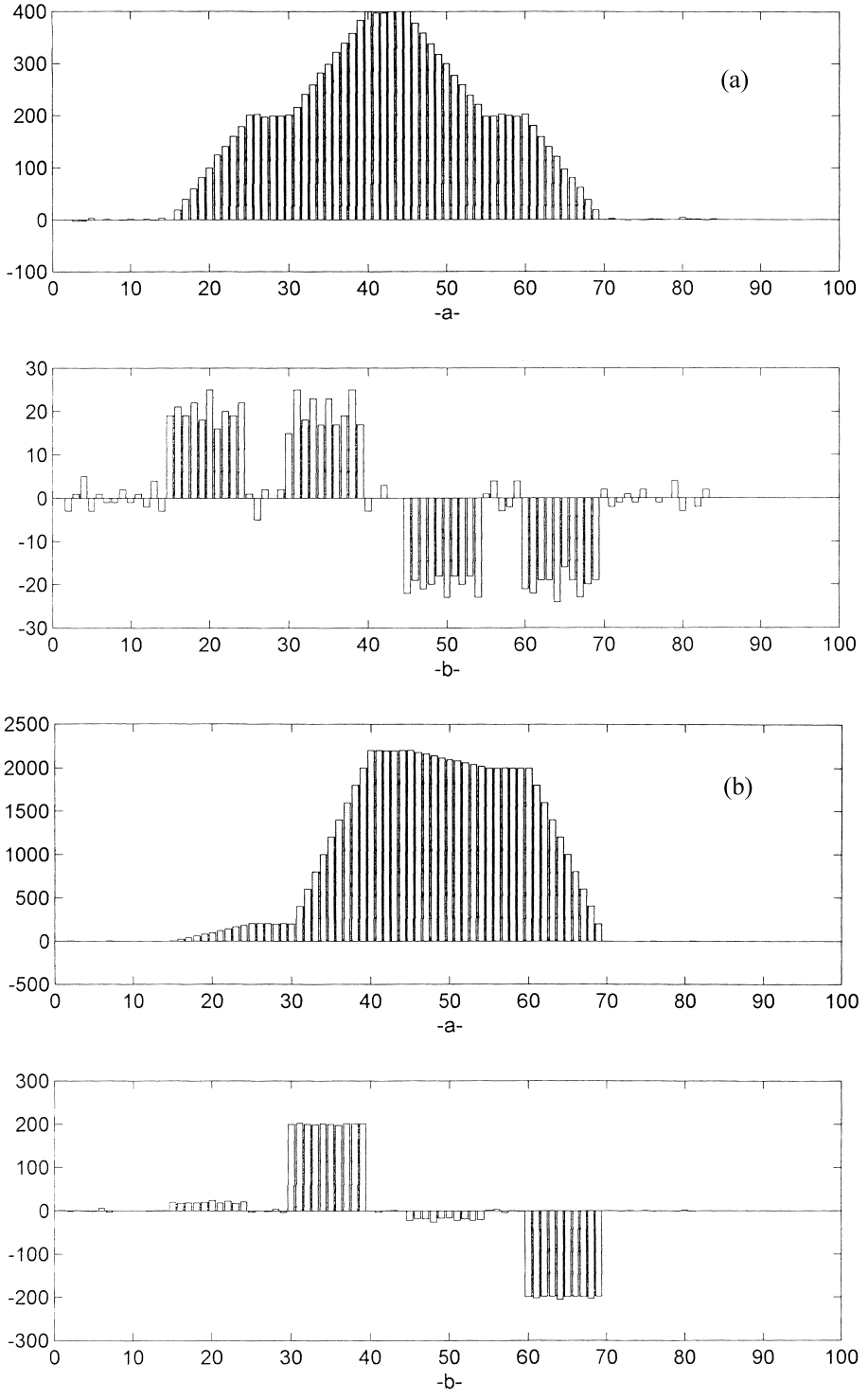

Fig. 13. As Fig. 12 except for $tdel = 15Ts$ ($ta < tdel < 2ta$).

two pulses by the first leading edge and the last trailing one, respectively, is yet easier and more exact.

3. $2ta < tdel < tb$.

   The first and the last flat top levels are the true ones of the two piling pulses. The second flat top level is no longer equal to the sum of the other two flat top levels (Fig. 11c and d), and pile up does not deteriorate just the first leading edge and the last trailing one.

4. $tdel = tb$.

   If the two piling signals are of equal amplitude (Fig. 14a), the amplitude of the piled signal is equal to the amplitude of each piling signal. The piled signal flat top width is equal to $2Tft + Tr$ while the piled signal width is equal to $2Tft + 3Tr$.

   On the contrary (Fig. 14b), the two flat top levels of the piled signal are the true ones of the two piling pulses. Pile up does not deteriorate just the first leading edge and the last trailing one.

5. $tb < tdel < tc$.

   The two flat top levels of the piled signal are distinctly separated from each other (Fig. 10c), the time distance becoming still more marked as delay increases. As for the rest, considerations analogous to the previous point ones apply.

6. $tdel < ta$.

   The piled up signal shows only a flat top (Fig. 15a). The edges are distorted assuming a shape which may well be approximated by different slope consecutive line segments. The flat top level of the piled signal is equal to the sum of the flat top ones of the two piling signals. The flat top level of the second signal must then be computed by subtracting the value of the first signal flat top level from the sum one. If the two piling signals are sufficiently spaced out, the first pulse amplitude-time information may be obtained by the least squares line representing the first line segment.

In the case the trapezoidal signal shown in Fig. 2b is shaped from a charge preamplifier with 10 ns rise time step output signal, the above procedure may be simplified though to the detriment of the measurement precision. In fact, the first level amplitude may directly be computed by the mean value of the first cluster of points (at minimum 2 points for $tdel = 4Ts$, at maximum 7 points for $tdel = 9Ts$) belonging to the first step level from the preamplifier (Fig. 15b). To reduce the standard deviation of the second level, this level is computed by subtracting the previous estimated first level amplitude from the flat top level of the signal at the output of the filter rather than from the mean value of the sum level points from the preamplifier, the standard deviation of the estimation being so essentially determined by the first level one.

For instance, from a typical measurement involving the pile up of two noisy (noise std = 4LSB) signals with $tdel = 5Ts$ and equal, low amplitudes (100LSB), the mean values of the first level, the sum level, the flat top level result in 95, 198.83, 199.16LSB with standard deviations of 4.58, 3.01, and 0.49LSB, respectively.

When $tdel \leq 3Ts$, the pile up situation is always revealable, but the first signal amplitude cannot be measured. By rejecting pulses for which the previous condition is verified, the percent counting loss is about 1.5, 3, 4, and 6 for a mean counting rate of 1, 2, 3, and 4 Mcps, respectively.

3. Conclusions

The trapezoidal shape originally implemented to overcome the ballistic deficit drawback in semiconductor gamma ray spectrometry, reveals itself useful in different experimental circumstances.

The shape synthesis digital technique allows time-amplitude measurement to be executed simply on real signals without any conceptual or experimental simplifying, also in the case of piled up pulses which is the usual one at high counting rate. Neither trigger nor pile up inspector circuit are needed when handling piled up pulses.

Programmability of both the leading and trailing edge slopes as well as the flat top width makes the shape usable in a wide range of spectrometric measurements. The flat top optimum quality is very important either to locate the zero and the non-zero clusters by the derivative signal or to compute the event energy without uncertainty except for the statistical one.

Modularity and flexibility of our acquisition parallel instrumentation results in useful properties in measurements by analog GI systems, systems em-

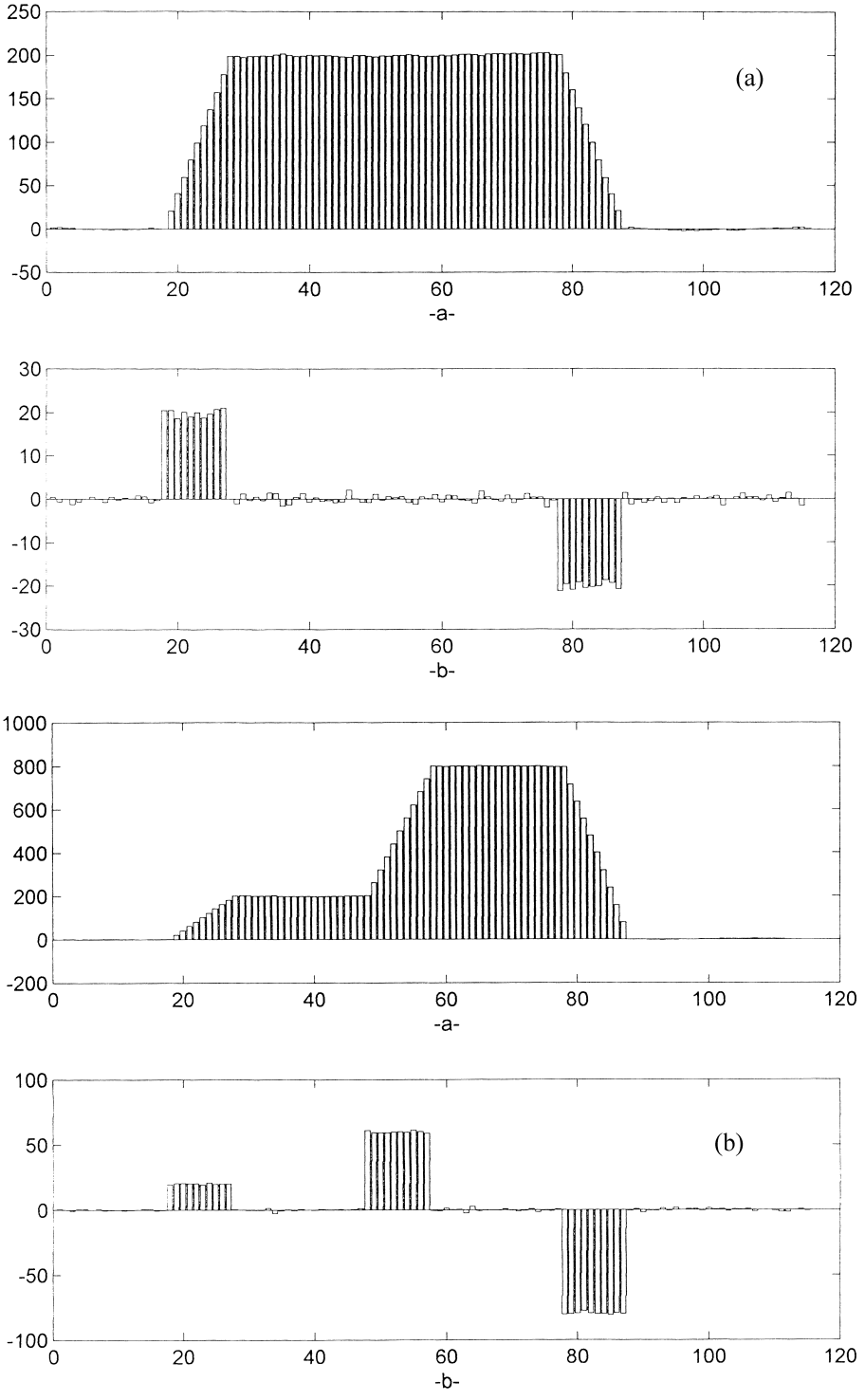

Fig. 14. As Fig. 12 except for *tdel* = *tb* = 30*Ts*.

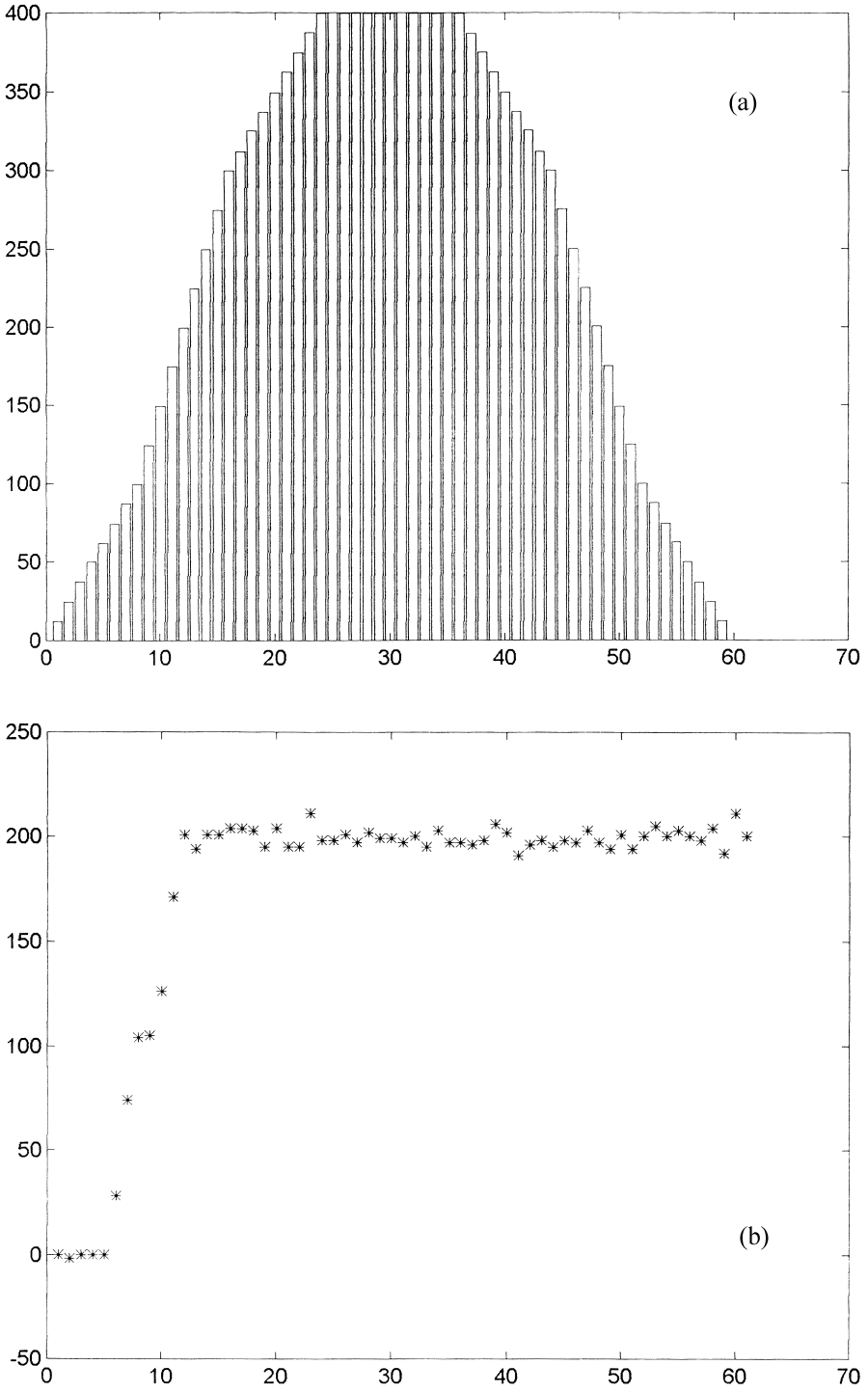

Fig. 15. First order pile up with *tdel* < *ta*. (a) Shows a trapezoidal shaper output. (b) Shows a preamplifier step output.

ploying digital integration of shortened pulse, and in the proposed all digital system.

In the first type of system, a pile up free pulse is usually shortened and integrated. A TAC starts on a timing pulse from one detector; a timing pulse from the opposite detector will stop the TAC. One ADC in the instrumentation reads the TAC level so determining the time interval between the two events, and one ADC for each detector reads the event energy from the level of the integrated energy signal. By modularity, the TOF measurement may be extended to more than one opposite detector [49].

In the second type of system, the shortened signal is sampled in the time interval between a start pulse and a stop one, both depending on the pile up free signal width. By modularity, the sampling frequency may be increased by increasing the number of ADC (for each ADC, the minimum sampling interval is equal to 25 ns) and integration methods more refined than the simple sample amplitude sum may be employed.

Modularity plays an analogous part in the all digital system which handles piled up pulses recovering the majority of them.

References

[1] C.L. Britton et al., Characteristics of high rate energy spectroscopy systems using HPGe coaxial detectors and time-variant filters, IEEE Trans. Nucl. Sci. 31 (1) (1984) 455.
[2] V. Radeka, Trapezoidal filtering of signals from large germanium detectors at high rates, IEEE Trans. Nucl. Sci. 19 (1972) 412.
[3] M. Cisotti et al., Transversal filter approach of trapezoidal pulse shaping for silicon live targets, Nucl. Instrum. Methods 159 (1979) 235.
[4] F.S. Goulding et al., GAMMASPHERE — elimination of ballistic deficit by using a quasi-trapezoidal pulse shaper, IEEE Trans. Nucl. Sci. 41 (4) (1994) 1140.
[5] K. Husimi, S. Ohkawa, Trapezoidal filtering of signals realized by the directly synthesized Gaussian filter, IEEE Trans. Nucl. Sci. 36 (1) (1989) 396.
[6] G. White, Pulse processing for gamma ray spectrometry. A novel method and its implementation, IEEE Trans. Nucl. Sci. 35 (1) (1988) 125.
[7] B.W. Loo, F.S. Goulding, Ballistic deficits in pulse shaping amplifiers, IEEE Trans. Nucl. Sci. 35 (1) (1988) 114.
[8] F.S. Goulding, D.A. Landis, Ballistic deficit correction in semiconductor detector spectrometers, IEEE Trans. Nucl. Sci. 35 (1) (1988) 119.
[9] M.L. Simpson et al., Charge trapping correction in Ge spectrometers, IEEE Trans. Nucl. Sci. 36 (1) (1989) 260.
[10] S.M. Hinshaw, D.A. Landis, A practical approach to ballistic deficit correction, IEEE Trans. Nucl. Sci. 37 (2) (1990) 374.
[11] F.S. Goulding, D.A. Landis, S.M. Hinshaw, Large coaxial germanium detectors — correction for ballistic deficit and trapping losses, IEEE Trans. Nucl. Sci. 37 (2) (1990) 417.
[12] M.L. Simpson et al., High-rate and high-energy gamma-ray spectroscopy using charge trapping and ballistic deficit correction circuits, IEEE Trans. Nucl. Sci. 37 (2) (1990) 444.
[13] J. Gal et al., Particle discriminator for the identification of light charged particles with CsI(Tl) scintillator + PIN photodiode detector, Nucl. Instrum. Methods A366 (1995) 120.
[14] Gy. Mathe, Method for the elimination of superposed pulses in nuclear spectroscopy, Nucl. Instrum. Methods 23 (1963) 261.
[15] E. Fuschini, C. Maroni, P. Veronesi, A circuit for rejecting pile up pulses, Nucl. Instrum. Methods 41 (1966) 153.
[16] M. Moszynski, J. Jastrzebski, B. Bengtson, Reduction of pile up effects in time and energy measurements, Nucl. Instrum. Methods 47 (1967) 61.
[17] F.S. Goulding, D.A. Landis, N.W. Madden, Design philosophy for high resolution rate and throughput spectroscopy systems, IEEE Trans. Nucl. Sci. 30 (1) (1983) 301.
[18] M. Sampietro et al., A digital system for optimum resolution in X-ray spectroscopy, Rev. Sci. Instrum. 66 (2) (1995) 975.
[19] G. Ripamonti, A. Geraci, Towards real-time digital pulse processing based on least mean squares algorithms, Nucl. Instrum. Methods A400 (1997) 447.
[20] A. Fazzi, V. Varoli, A digital spectrometer for optimum pulse processing, IEEE Trans. Nucl. Sci. 45 (3) (1998) 843.
[21] J.E. Dennis, D.M. Gay, R.E. Welsch, An adaptive nonlinear least-squares algorithm, ACM Trans. Math. Softw. 7 (3) (1981) 348.
[22] D.G. Politte, Image improvements in positron-emission tomography due to measuring differential time-of-flight and using maximum likelihood estimation, IEEE Trans. Nucl. Sci. 37 (2) (1990) 737.
[23] D.R. Haynor, R.L. Harrison, T.K. Lewellen, A scheme for accidental coincidence correction in time-of-flight positron tomography: theory and implementation, IEEE Trans. Nucl. Sci. 35 (1) (1988) 753.
[24] T.J. Holmes, Predicting count loss in modern positron emission tomography systems, IEEE Trans. Nucl. Sci. 30 (1) (1983) 723.
[25] G. Germano, E.J. Hoffman, A study of data loss and mispositioning due to pile up in 2-D detectors in PET, IEEE Trans. Nucl. Sci. 37 (2) (1990) 671.
[26] P.E. Kinahan, J.S. Karp, Position estimation and error correction in a 2-D position sensitive NaI(Tl) detector, Nucl. Instrum. Methods A299 (1990) 484.
[27] L. Lyons, W.W.M. Allison, J. Panella Comellas, Maximum likelihood or extended maximum likelihood? An example from high energy physics, Nucl. Instrum. Methods A245 (1986) 530.
[28] W.R. Cook, M. Finger, T.A. Prince, A thick Anger camera

for gamma ray astronomy, IEEE Trans. Nucl. Sci. 32 (1) (1985) 129.
[29] C.T. Roche, M.G. Strauss, R. Brenner, Resolution and linearity of Anger-type neutron-position detectors as simulated with different signal processing and optics, IEEE Trans. Nucl. Sci. 32 (1) (1985) 373.
[30] T.D. Milster et al., Digital position estimation for the modular scintillation camera, IEEE Trans. Nucl. Sci. 32 (1) (1985) 748.
[31] N.H. Clinthorne et al., A hybrid maximum likelihood position computer for scintillation cameras, IEEE Trans. Nucl. Sci. 34 (1) (1987) 97.
[32] A.O. Hero, N.H. Clinthorne, W.L. Rogers, A lower bound on PET timing estimation with pulse pileup, IEEE Trans. Nucl. Sci. 38 (2) (1991) 709.
[33] N. Petrick et al., Least squares arrival time estimators for photons detected using a photomultiplier tube, IEEE Trans. Nucl. Sci. 39 (4) (1992) 738.
[34] N. Petrick et al., Least squares arrival time estimators for single and piled up scintillation pulses, IEEE Trans. Nucl. Sci. 40 (4) (1993) 1026.
[35] N. Petrick et al., A fast least squares arrival time estimator for scintillation pulses, IEEE Trans. Nucl. Sci. 41 (4) (1994) 758.
[36] F. Hilsenrath, H.D. Voss, J.C. Bakke, A single chip pulse processor for nuclear spectroscopy, IEEE Trans. Nucl. Sci. 32 (1) (1985) 145.
[37] J.S. Karp et al., Event localization in a continuous scintillation detector using digital processing, IEEE Trans. Nucl. Sci. 33 (1) (1986) 550.
[38] G. Amsel, R. Bosshard, C. Zajde, Shortening of detector signals with passive filters for pile up reduction, Nucl. Instrum. Methods 71 (1969) 1.
[39] J.A. Wear et al., A model of the high count rate performance of NaI(Tl)-based PET detectors, IEEE Trans. Nucl. Sci. 45 (3) (1998) 1231.
[40] R. Freifelder et al., Comparison of multi-pole shaping and delay line clipping preamplifiers for position sensitive NaI(Tl) detectors, IEEE Trans. Nucl. Sci. 45 (3) (1998) 1138.
[41] E. Tanaka, N. Nohara, H. Murayama, Variable sampling time technique for improving count rate performance of scintillation detectors, Nucl. Instrum. Methods 158 (1979) 459.
[42] M. Kastner, A high speed stabilized gated integrator, IEEE Trans. Nucl. Sci. 31 (1) (1984) 447.
[43] M. Bentourkia et al., Object and detector scatter function dependence on energy and position in high resolution PET, IEEE Trans. Nucl. Sci. 42 (1995) 1162.
[44] V. Drndarevic, P. Ryge, T. Gozani, Digital signal processing for high rate gamma-ray spectroscopy, Nucl. Instrum. Methods A277 (1989) 532.
[45] T.K. Wellem et al., A new clinical scintillation camera with pulse tail extrapolation electronics, IEEE Trans. Nucl. Sci. 37 (2) (1990) 702.
[46] W.H. Wong, H. Li, A scintillation detector signal processing technique with active pile up prevention for extending scintillation count rates, IEEE Trans. Nucl. Sci. 45 (2) (1998) 838.
[47] S. Bittanti et al., High-accuracy fit of the poles of spectroscopy amplifiers designed for mixed analog-digital filtering, IEEE Trans. Nucl. Sci. 44 (2) (1997) 125.
[48] C.H. Reinsch, Smoothing by spline functions, Numer. Math. 10 (1967) 177.
[49] C. Imperiale, A. Imperiale, Some fast mono multi-processor configurations for a single multi-parameter multichannel analyzer, Measurement 27 (2000) 257.
[50] F.S. Goulding, D.A. Landis, GAMMASPHERE — correction techniques for detector charge trapping, IEEE Trans. Nucl. Sci. 41 (4) (1994) 1145.
[51] M. Moszynski, B. Bengtson, The shape distribution of pulses from a planar Ge(Li) detector studied by a differential pulse-shape selection method, Nucl. Instrum. Methods 100 (1972) 285.
[52] T.W. Raudorf et al., Comparative timing performance of large volume Ge(Li) and HPGE coaxial detectors, IEEE Trans. Nucl. Sci. 24 (1) (1977) 78.
[53] T.W. Raudorf et al., Pulse shape and risetime distribution calculations for HPGe coaxial detectors, IEEE Trans. Nucl. Sci. 29 (1) (1982) 764.
[54] F.S. Goulding, Pulse-shaping in low noise nuclear amplifiers: a physical approach to noise analysis, Nucl. Instrum. Methods 100 (1972) 493.